International Journal of Advanced Science and Technology
Vol. 28, No. 16, (2019), pp. 792 - 811

Optimization of Robust and LQR Control Parameters for Half Car Model using Genetic Algorithm

Mohammed Kaleemullah[1], Waleed F Faris[2], FariedHasbullah, Nouby M. Ghazaly[3]
[1]*Department of Electronics & Communication Engineering, C. Abdul Hakeem College of Engineering and Technology, Vellore, Tamil Nadu, India*
[2]*Faculty of Engineering, International Islamic University Malaysia, Kuala Lumpur, Malaysia*
[3]*Mechanical Engineering Dept., Faculty of Engineering, South Valley University, Qena-83521, Egypt*
waleed@iium.edu.my, mkalim@gmail.com

Abstract

To test the performance of the half car system, two types of controller are used, namely Robust H-infinity control and LQR control. Robust H-infinity and LQR controller is designed to control the suspension system and to reduce the vibrations in the car and to improve handling. A half car model is considered in this research to study the effects in passenger owing to different road profiles. The weights of Robust H-infinity and LQR controller are obtained using Genetic Algorithm on a half car model with two different types of usually existing road disturbance.The design parameters of both the active controller varies with various road profiles. This proves that particular design parameters in Robust and LQR controller do not have the ability to adapt to the variations in road surface. Furthermore, active controllers significantly improve the performance of the system in all aspects when compared to passive system.

1. Introduction

Suspension system is the main tool to achieve ride comfort and vehicle control. The design of passive suspension has always been focused on obtaining a good compromise between these two goals. However, structural limitations prevent passive suspension from achieving the best performances for both targets. For example, soft springs facilitate good ride characteristics at the expense of increased wheel motion and increased variations in dynamic tire loadings on rough roads. On the other hand, good road handling characteristics and smaller wheel motion is an attribute of larger spring rates. Thus, spring rates should be chosen large enough to limit wheel motion and dynamic tire variations but small enough to provide a comfortable ride[1]. As pointed by Barr and Ray[1], the choice and arrangement of the elements of passive suspension has evolved into a near optimal design through many years of experimentation and testing.

Active suspension system has the capability to continuously adjust itself, hence has a better design trade-offs compared to a conventional suspension system. The desired additional force in active suspension system is usually employed by hydraulic or pneumatic actuators which are secured in parallel with a spring and damper. The amount of force required for the actuators are controlled by the controller based on the motions of the vehicle which is received from various sensors located at different points of the vehicle[2-4].

Vehicle response to excitations is usually modelled in two approaches. First approach is using discrete modelling. This approach breaks down the car into lumped systems of masses, springs, and dampers,which is the most popular among researchers due to its simplicity and it is argued that it gives reasonable results with minimum computation effort (Wong, 2008). The second approach is using what is known in dynamics as continuous modelling. In this approach, the car is taken completely including its geometry into consideration. The main tool for this approach is Finite Element Method. This approach is becoming popular in industries but the main disadvantages are the computational effort and the need for an expertise in using FEM. As mentioned earlier, discrete system approach is still the most common among researchers.

Stone [5]have described a detail derivation of a full car vehicle model with 6-DOF using the Newtonian approach. This model is able to simulate the effect of suspension (ride) as well as braking and steering (handling) in all three translational motions (vertical, forward and side), pitch, roll and yaw (heave) directions. General assumptions in deriving the model are the vehicle mass could be lumped into a single mass which is referred to as the sprung mass, the vehicle centre of gravity is located above the roll and pitch centres, the vehicle suspension springs will not be allowed to *top out* during manoeuvring; the suspension springs will always be in compression, aerodynamic lift and drag force, and tire rolling resistance are neglected, the vehicle remains grounded at all times, i.e. the four tires never lose contact with the ground, and the deflections in the pitch and roll planes are small, and may be simplified with small angle approximation.

Gillespie [6]studied quarter car model under the effect of road roughness. They found that quarter car models to be adequate for discriminating the roughness of the road on a scale that correlates well to the public judgment of its severity.

Solimon[7]aimed at introducing a solution of the vehicle dynamics problem by studying the effect of various types of suspension element on the vehicle suspension system performance. They derived mathematical models of conventional quarter car model, quarter car model with twin spring system, quarter car fully active system and half car conventional model and conducted experiment to verify the theoretical analysis. They concluded that load carrying capacity of a vehicle rear suspension can be solved using stiff suspension spring system or a twin spring suspension system, a fully active suspension system can improve the vehicle performance criteria significantly but at a high cost, the tire damping has a very small effect on the vehicle ride comfort, when the tire stiffness parameter is increased, the systems have higher wheel resonance peaks in the dynamic tire load response, the predicted values of the suspension working space and vertical acceleration were 8 – 10% lower than the measured, and the peak resonance for the body acceleration and suspension working space at a certain frequency was similar to that obtained theoretically.

Most of the work carried out in Robust H_∞ control is focused in Quarter car model. The advantage of quarter car model is: simpler to analyze and model but it is limited to only being able to simulate vertical deflection of the car. Due to this, the effect of pitch cannot be determined and analyzed. The goal of this research is categorized into the following: vehicle control performance and passengers ride comfort. Robust H-infinity and LQR controller is designed to control the suspension system and to reduce the vibrations in the car and to improve handling. A half car model is considered in this research to study the effects in passenger owing to different road profiles. The weights of Robust H-infinity and LQR controller are obtained using Genetic Algorithm on a half car model with different types of usually existing road disturbance. The investigation was carried out in time domain of the system. In this work, the dynamics of the actuator is not taken into account and the system is considered linear.

2. Vehicle Modeling

A model generally represents an approximation of the actual physical system which can be modelled in different ways. However, a good system model must include all the important dynamic characteristics of the system so that the response achieved by the model could satisfactorily match the behaviour of the actual system.

Modelling in vibration can be categorized into two types – lumped parameter system (discrete system) and distributed parameter system (continuous system). In this work, discrete modelling of system is considered which describes vehicle as lumped mass or finite degree of freedom system.

To study ride quality, vehicle mass is usually separated into two – sprung mass (vehicle body) and unsprung mass (vehicle wheel). Unsprung mass includes mass of tire, brakes, suspension linkages and other mass associated with the wheel. This part of the vehicle is on the roadside and thus reacts to irregular road profile with no damping.

The two axle four degree-of-freedom model used in this study is shown in the Figure 1**Error! Reference source not found.**. The four DOFs are, sprung mass vertical displacement (x_s), sprung mass pitch (θ), front unsprung mass displacement (x_{uf}) and rear unsprung mass displacement (x_{ur}). One of the inputs to the considered linear model is the displacement which represents a typical road profile. This input from the road surface excites the unsprung mass which corresponds to suspension components, wheel and tire. The unsprung mass is connected to the sprung mass which represents the body of vehicle through spring, damper and actuator. The equation of motion of the half car system can be derived as

$$m_s \ddot{x}_s + k_{sf}(Z_f) + k_{sr}(Z_r) + c_{sf}(\dot{Z}_f) + c_{sr}(\dot{Z}_r) - f_f - f_r = 0 \tag{1}$$

$$I_{yy}\ddot{\theta} - k_{sf}(Z_f)a + k_{sr}(Z_r)b - c_{sf}(\dot{Z}_f)a + c_{sr}(\dot{Z}_r)b + f_f a - f_r b = 0 \tag{2}$$

$$m_{uf}\ddot{x}_{uf} - k_{sf}(Z_f) - c_{sf}(\dot{Z}_f) + k_{tf}(x_{uf} - x_{rf}) + f_f = 0$$

(Error! No text of specified style in document.)

$$m_{ur}x_{ur} - k_{sr}(Z_r) - c_{sr}(\dot{Z}_r) + k_{tr}(x_{ur} - x_{rr}) + f_r = 0 \tag{4}$$

International Journal of Advanced Science and Technology
Vol. 28, No. 16, (2019), pp. 792 - 811

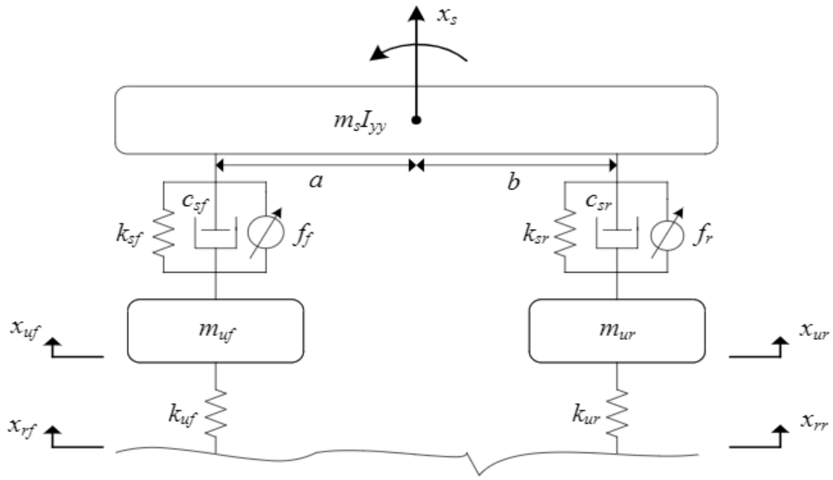

Figure 1. Four Do F half car model

where

$$Z_f = x_s - a\theta - x_{uf}$$

$$Z_r = x_s + b\theta - x_{ur}$$

These equations of motion can be described in state space form as

$$\dot{X} = Ax + Bu + Gw \tag{5}$$

where state vectors x represents the controlled input, u represents the actuator input and w represents the road disturbance,

$$x = [x_s \quad \theta \quad x_{uf} \quad x_{ur} \quad \dot{x}_s \quad \dot{\theta} \quad \dot{x}_{uf} \quad \dot{x}_{ur}]^T$$

$$u = \begin{bmatrix} f_f \\ f_r \end{bmatrix}$$

$$w = \begin{bmatrix} x_{rf} \\ x_{rr} \end{bmatrix}$$

The interested output state variable are sprung mass vertical acceleration $(\ddot{x}_s)$, sprung mass pitch angular acceleration $(\ddot{\theta})$, front suspension deflection $(x_s - a\ddot{\theta} - x_{uf})$, rear suspension deflection $(x_s + b\ddot{\theta} - x_{ur})$, front tire deflection $(x_{uf} - x_{rf})$ and rear tire deflection $(x_{ur} - x_{rr})$.

The output of the system is written as

$$y = Cx + Du + Hw \tag{6}$$

The state variable descriptions and vehicle nominal model parameters values are provided in Table 1 and Table 2 respectively.

ISSN: 2005-4238 IJAST

Table 1: State variables and input description for half car

Symbol	Parameters
x_s	m_s displacement (m)
θ	m_s pitch (rad)
x_{uf}	m_{uf} displacement (m)
x_{ur}	m_{ur} displacement (m)
x_{rf}	Front input (m)
x_{rr}	Rear input (m)

Table 2. Model parameters of half car

Symbol	**Description**	**Nominal Value**	**unit**
m_s	Sprung mass	730	kg
I_{yy}	Pitch moment of inertia	2460	kgm^2
m_{uf}	Front unsprung mass	40	kg
m_{ur}	Rear unsprung mass	40	kg
a	Distance from ms CG to front	1.011	m
b	Distance from ms CG to rear	1.803	m
k_{sf}	Front suspension stiffness	19960	N/m
k_{sr}	Rear suspension stiffness	17500	N/m
k_{tf}	Front tire stiffness	175500	N/m
k_{tr}	Rear tire stiffness	175500	N/m
c_{sf}	Front suspension damping coefficient	1290	N s/m
c_{sr}	Rear suspension damping coefficient	1620	N s/m

3. Disturbance Modeling

As discussed earlier, vehicle ride and handling are influenced mainly by two sets of disturbance. One is caused by different forces that originate due to braking, turning and wind gusts for instance and the other is due to road roughness. The more significant of the two types is the input disturbance from road surface.

The input from road surface can be broadly classified as shock and vibration. Shocks are nothing but discreet event of relatively short duration but high intensity, such as the disturbance caused by a bump or pothole on a smooth road profile. However, vibrations are characterized by prolonged and consistent disturbance that are felt on rough road [8]. These geometric irregularities of the road play a major role in causing vehicle vibration, which directly influence vehicle wear, ride comfort and safety. In order to understand the seriousness of uneven surface, road profile and its roughness have to be measured and classified before the analysis. The designers develop vehicles for varied application by referring to the condition of the road [9].

3.1. Random Disturbance

Road roughness is an important factor as an indicator of road condition in terms of road pavement performance and as a determinant of road user cost. Road profiles fit in the category of "broad-band random signals" and thus can be described by both as a profile or its statistical properties. Power Spectral Density (PSD) is highly used to represent random road disturbance. Nevertheless, other properties of random signals such as stationary and ergodic are also used to describe road profile.

It is found that the relation between the power spectral density and the spatial frequency for the road profile can be approximated by

$$S_g(\Omega) = C_{sp}\Omega^{-N} \tag{1}$$

where, $S_g(\Omega)$ is the PSD of the elevation of the surface profile, and C_{sp} and N are constants. A typical measured spectral densities of various terrains by [10] using the above Equation (1) is shown in the Figure 2, with its corresponding values in Table 3.

Over the years, various organizations have made attempts to classify the road irregularities. The international Organization for Standardization (ISO) has proposed road irregularities classification based on power spectral density (PSD) as shown in Table 4 and Figure shows the classification of roads proposed by ISO [11].

Table 3: Values of C_{sp} and N for PSD for various surfaces [10]

Description	***N***	***C_{sp}***
Smooth runway	3.8	4.3×10^{-11}
Rough runway	2.1	8.1×10^{-6}
Smooth highway	2.1	4.8×10^{-11}
Highway with gravel	2.1	4.4×10^{-11}
Pasture	1.6	3×10^{-4}
Plowed field	1.6	6.5×10^{-4}

ISSN: 2005-4238 IJAST

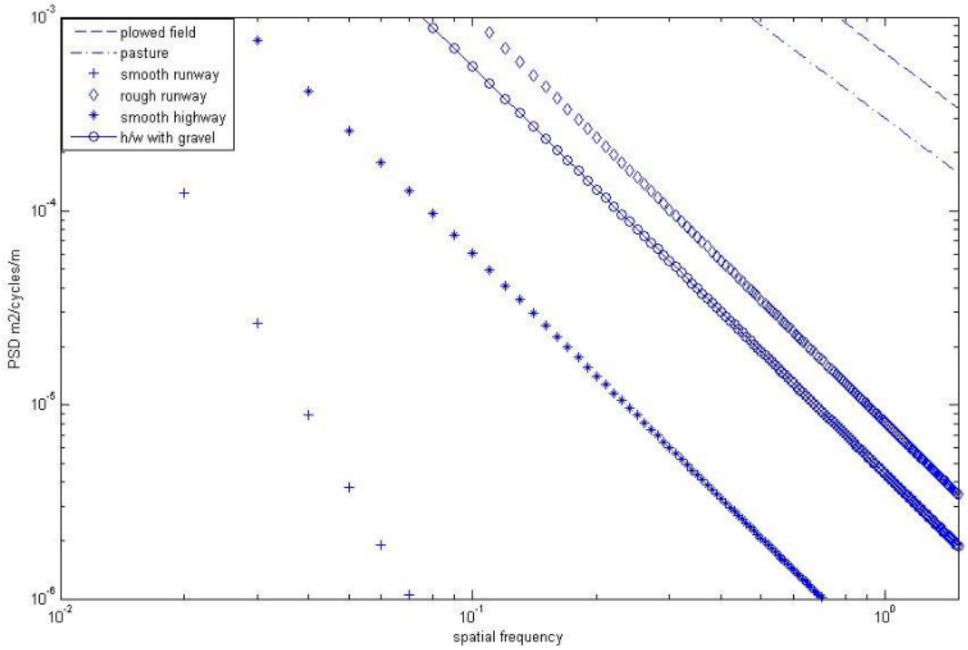

Figure 2: Power Spectral Density for various types of road and runways

The relationship between PSD $S_g(\Omega)$ and the spatial frequency Ω for different road roughness can be approximated by

For $\Omega \le \Omega_o = 1/2\pi$ cycles/m,

$$S_g(\Omega) = S_g(\Omega_o)\,(\Omega/\Omega_o)^{-N1} \tag{2}$$

For $\Omega > \Omega_o = 1/2\pi$ cycles/m,

$$S_g(\Omega) = S_g(\Omega_o)\,(\Omega/\Omega_o)^{-N2} \tag{3}$$

Table 4, shows the range of values of $S_g(\Omega_o)$ at a spatial frequency $\Omega_o = 1/2\pi$ cycles/m for different classes of road. The values of N_1 and N_2 are 2 and 1.5 respectively.

Table 4: ISO classification of road roughness

	Degree of roughness $S_g(\Omega_o)$, 10^{-6} m^2/cycles/m	
Road Class	Range	Geometric Mean
A (very good)	<8	4
B (good)	8 - 32	16
C(average)	32 - 128	64
D (poor)	128 - 512	256
E (very poor)	512 - 2048	1024
F	2048 - 8192	4096
G	8192 - 32,768	12288
H	>32,768	16384

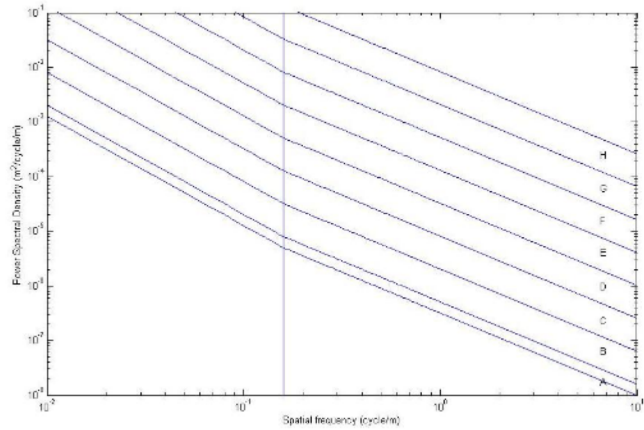

Figure 3: classification of road surface roughness by ISO

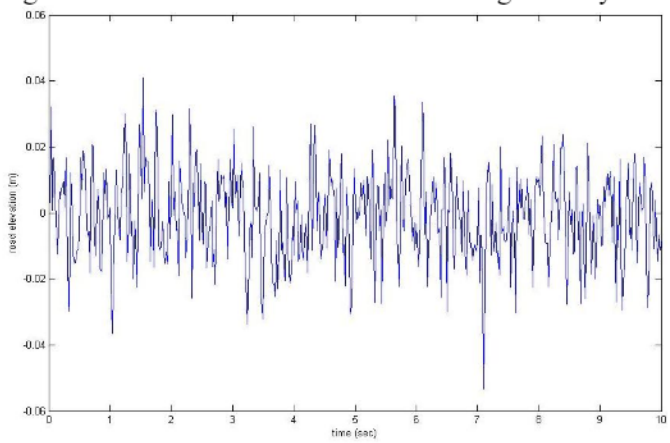

Figure 2: Random surface profile

Excitation from ground surface as shown in Figure 2 can be described using random disturbance more realistically. Equation (10), is used to describe random profile [12],

$$\dot{z}_r(t) + w_o z_r(t) = \sqrt{S_g(\Omega_o)u}\,.\,w(t) \tag{4}$$

Where $z_r(t)$ is the road profile, $w(t)$ is a white noise, w_o is equal to $0.2\,\pi\,u$, with u as the velocity of the vehicle and $S_g(\Omega_o)$ is the road roughness.

3.2. Pothole Input

A further study is performed on a more common road disturbance like bumps and potholes. Usually, these are the kind of disturbance which is more commonly faced by passenger on roads. The pothole disturbance used in this study is based on the pothole track at the Gerotek test facilities in South Africa which is 80 mm deep in the road. In the Figure 3, front disturbance is represented using line, while the dashed lined represents rear input after certain time delay.

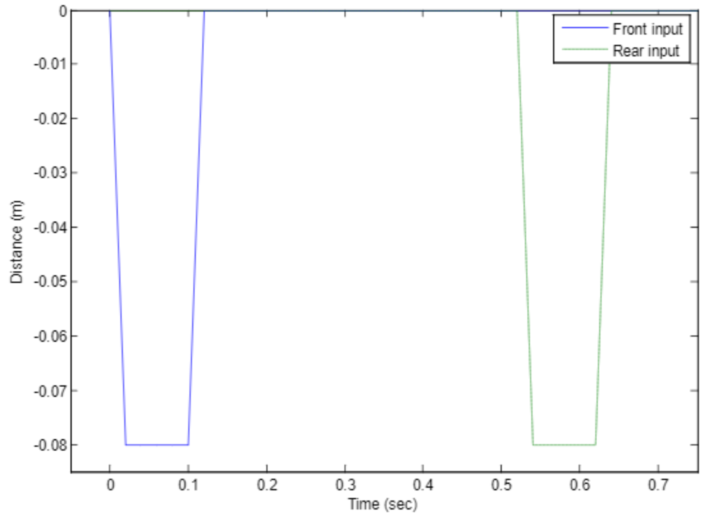

Figure 3: Pothole disturbance input

4. Controller Design

4.1. H-infinity Control Theory

Robust H_∞technique with nominal model and modelling uncertainty is considered due changing system parameters owing.

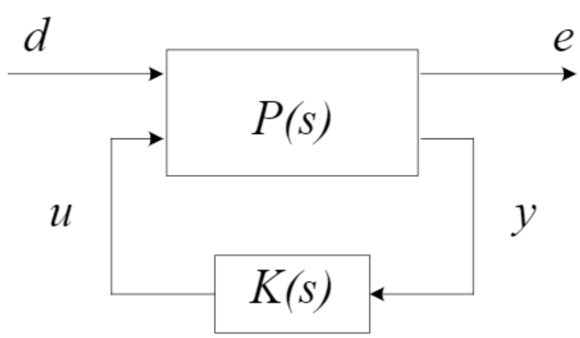

Figure 6: Robust controller K(s)

In Figure6*P(s)* is the generalized plant, d denotes all external disturbance, output signal is taken as error e which is to be minimized, y is the input to controller K and u is the vector of controlled signals which is also to be reduced to avoid the saturation of the actuator.

State space equation in the form as shown in Eq. (11) is used to represent the system shown in Figure6.

$$
\begin{aligned}
\dot{x} &= Ax + B_1 d + B_2 u \\
e &= C_1 x + D_{11} d + D_{12} u \\
y &= C_2 x + D_{21} d + D_{22} u
\end{aligned}
\tag{11}
$$

The above state space representation can be written in matrix form as,

ISSN: 2005-4238 IJAST

$$P(s) = \begin{bmatrix} A & B_1 & B_2 \\ C_1 & 0 & D_{12} \\ C_2 & D_{21} & 0 \end{bmatrix} \tag{12}$$

By taking lower LFT for the plant matrix *P(s),*

$$F_L(P,K) = P_{11} + P_{12}K(I - P_{22}K)^{-1}P_{21} \tag{13}$$

The goal of H-infinity controller is to find a stabilizing controller *K(s)* to minimize H-infinity norm of the closed loop transfer function is less than a given positive number, i.e.

$$\left\|T_{ed}\right\|_\infty = \left\|F_L\,(P,K)\right\|_\infty \tag{14}$$

We may obtain an optimal solution by successively reducing the value of γ from a large number [13]. It should be taken care that reducing γ more than the nominal range makes the solution unreliable [14]. Given an acceptable value of γ, we can compute a controller *K* such that,

$$\left\|F_L\,(P,K)\right\|_\infty < \gamma \tag{15}$$

The H_∞ controller can be found using two Ricatti equations by solving it iteratively [15].

$$A^T X_\infty + X_\infty a + C_1^T C_1 - \gamma^{-2} X_\infty B_1 B_1^T X_\infty - X_\infty B_2 B_2^T X_\infty = 0 \tag{16}$$

$$AY_\infty + Y_\infty A^T + B_1 B_1^T - \gamma^{-2} Y_\infty C_1^T C_1 Y_\infty - Y_\infty C_2^T C_2 Y_\infty = 0 \tag{17}$$

whereX_∞ and Y_∞ are the optimal solution of the Ricatti equations. In the Figure 7, $\Delta(s)$ represents the uncertain parameters of the system.

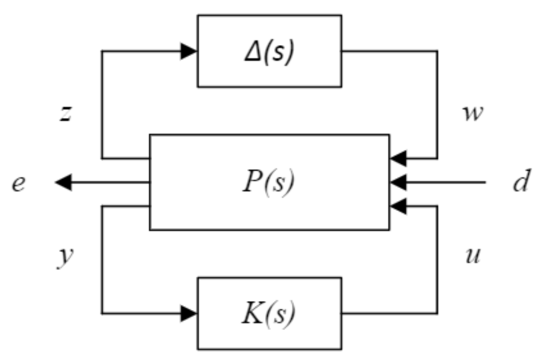

Figure 7: System with uncertainty

4.2. Weighting Function

Selecting an appropriate weighting function is one of the most important steps in the robust controller design. The weighting function W_d, W_n, W_p, W_a are included for the following reasons [16].

- To avoid saturation of the actuator W_a by constraining the magnitude of the input signal.
- To ensure good closed loop performance specification W_p
- To signify the frequency content of external disturbances and noises such as W_d and W_n respectively.

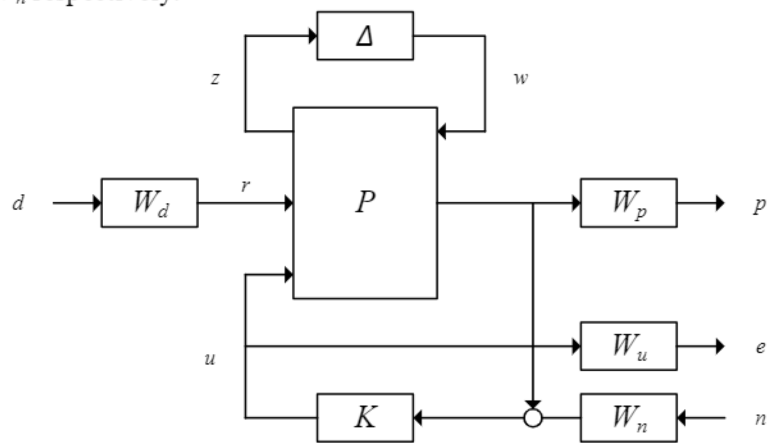

Figure 8. Closed loop system with uncertainty

It should be noted that the amplitude of the disturbance signal does not correspond to the actual external disturbance affecting the system. For instance, in figure (8), the norm of $\widetilde{d}$ must be less than or equal to 1 and the norm of d is less or equal to the maximum amplitude of the disturbance which may occur from improper road surface.

Sensor noise Wn= 0.02 is chosen for sprung mass vertical acceleration and pitch acceleration thus representing that the sensor noise is 0.02m/s^2. It is assumed that the sensor noise for the suspension deflection is 0.001 m/s^2. The front and rear weighting function for road disturbance are chosen as 0.05. Closed loop model of the system after adding uncertainty and weighting function is shown in figure (8).

5. LQR Controller

LQR control design model was adopted from [17]. While designing, it is assumed that all the states for the system described in equation (5) are available and can be measured. The LQR control was designed to minimize the following output weighted performance index are positive definite diagonal weighting matrices to emphasize the appropriate output of interest and control signal respectively.

$$\boldsymbol{J} = \int_0^{\infty} (\mathbf{y}^{\mathrm{T}}\mathbf{Q}\mathbf{y} + \rho\mathbf{u}^{\mathrm{T}}\mathbf{R}\mathbf{u}))dt \tag{18}$$

where

$$\mathbf{Q} = \begin{pmatrix} q_1 & 0 & 0 \\ 0 & \ddots & 0 \\ 0 & 0 & q_n \end{pmatrix}_{n \times n} \tag{19}$$

$$\mathbf{R} = \begin{pmatrix} r_m & 0 & 0 \\ 0 & \ddots & 0 \\ 0 & 0 & r_m \end{pmatrix}_{m\times m} \tag{20}$$

In the above equation, y is the output of interest, n is the number of output and m is the number of controller output. The role of ρ is to create a trade-off between the controlled output and the control signal.

The index can be rewritten as

$$\boldsymbol{J} = \int_0^\infty (\mathbf{x}^T\overline{\mathbf{Q}}\mathbf{x} + \mathbf{u}^T\overline{\mathbf{R}}\mathbf{u} + 2\mathbf{x}^T\overline{\mathbf{N}}\mathbf{u})dt \tag{21}$$

where

$$\overline{\mathbf{Q}} = \mathbf{C}^T\mathbf{Q}\mathbf{C} \tag{22}$$

$$\overline{\mathbf{R}} = \mathbf{D}^T\mathbf{Q}\mathbf{D} + \rho\mathbf{R} \tag{23}$$

and

$$\overline{\mathbf{N}} = \mathbf{C}^T\mathbf{Q}\mathbf{D} \tag{24}$$

The required optimal state feedback LQR control can be established using the state feedback law

$$\mathbf{u} = \mathbf{-Kx} \tag{25}$$

where$K$ is given by

$$\mathbf{K} = \mathbf{R}^{-1}(\mathbf{B}^T\mathbf{P} + \mathbf{N}^T) \tag{26}$$

here, P is obtained using the solution of Algebraic Ricatti Equation (ARE).

$$\mathbf{A}^T\mathbf{P} + \mathbf{P}\mathbf{A} + \overline{\mathbf{Q}} - (\mathbf{P}\mathbf{B} + \overline{\mathbf{N}})\overline{\mathbf{R}}^{-1}(\mathbf{B}^T\mathbf{P} + \overline{\mathbf{N}}^T) = 0 \tag{27}$$

$$\dot{\mathbf{x}} = (\mathbf{A} - \mathbf{B}\mathbf{K})\mathbf{x} + \mathbf{G}\mathbf{w} \tag{28}$$

The required elements of the Q and R matrices and the constant ρ are obtained using Genetic Algorithm.

6. Genetic Algorithm

Genetic Algorithm (GA) toolbox was used to find the actuator weighting function W_{af}, W_{ar} for front and rear actuator respectively and performance weighting function W_{p1} to W_{p6} for body vertical acceleration, pitch acceleration, suspension deflections, and tire deflections. Similarly GA is used to find the elements of the **Q**and**R**matrices and the constant ρ for LQR controller.

The idea behind this is that the GA creates series of new population of individuals or chromosomes in the existing generation that are used to produce the next population in subsequent steps:

a. Scores all individual member of the existing population by computing its fitness value and scales the raw scores to convert them into a more practical range of values.
b. Selects parents based on their fitness values.
c. Perform elitist selection, through which some of the better member of the current population are allowed to carry over to the next population unchanged.
d. Children are produced either by mutation or crossover.
e. Replaces the current population with that of children to form the next generation.

Figure 9: Flow chart of the algorithm

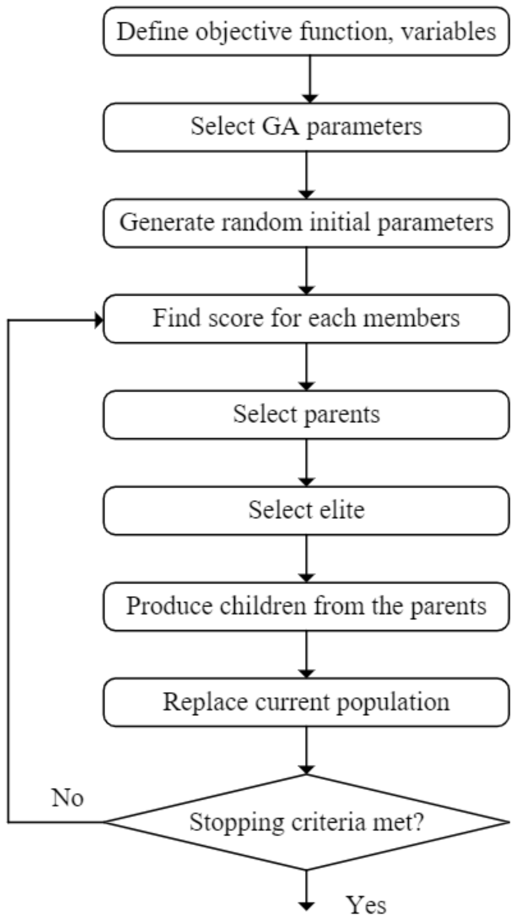

The algorithm stops when one of the criteria is met. The performance and actuator weighting functions for robust control are chosen as the individual to be optimized. Figure 9, shows flow chart of the algorithm.

6.1. Optimization Problem Formulation

To improve performance of the vehicle, the objective function was set to reduce sprung mass vertical acceleration, $\ddot{x}_s$ of the vehicle.

$$y_{ptp} = \max(y(t)) - \min(y(t)) \tag{29}$$

As the performance of the active suspension system is evaluated with passive system, the following constraints are considered

$$g_i = \frac{y_{a,i}}{y_{p,i}} \leq 1, i = 1,2,3, \dots, n \tag{30}$$

where
y_a = output of active suspension system
y_p = output of passive suspension system
n = number of outputs

By using the penalty approach, the constrained optimization problem is converted into unconstrained optimization problem. The modified objective for this approach is

$$f(1) = \ddot{x}_s + \rho \tag{31}$$

whereρ is the penalty and is given by

$$\rho = \begin{cases} \sum_{i=2}^{n} g_i, & if\, g_i > 1 \\ 0, & otherwise \end{cases} \tag{32}$$

7. Response to Pothole Input

7.1. Sprung Mass Acceleration

The summary of the result of sprung mass vertical acceleration's peak-to-peak and settling time due to pothole input is shown in Figure10 - Figure 11 respectively. The result shows that Robust H-infinity control improves the settling time performance by 50.4% when compared to passive system. In terms of peak-to-peak value, LQR controller improves the performance by 29.3% when compared to passive system. The active controllers prove to perform better than passive system in both the aspect.

Figure12 and Figure 13 shows the result of the sprung mass pitch acceleration. Even in this case, active controllers showed best results than passive system. From these results, it can be infer that, robust controller improves the performance of the PTP and settling time by 20.3% and 56.4% when compared with passive system respectively.

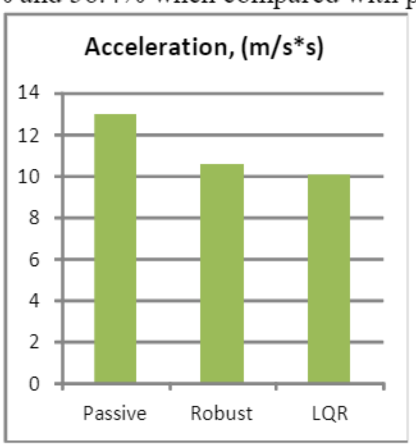

Figure10: PTP of sprung mass acceleration

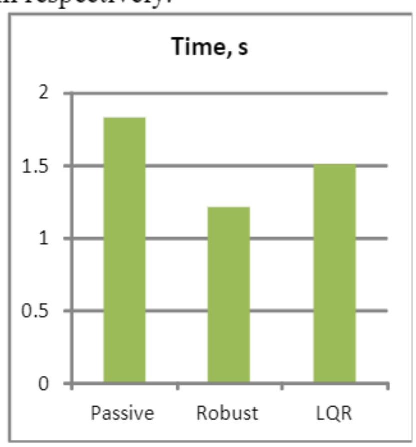

Figure 11: Settling time of sprung mass acceleration

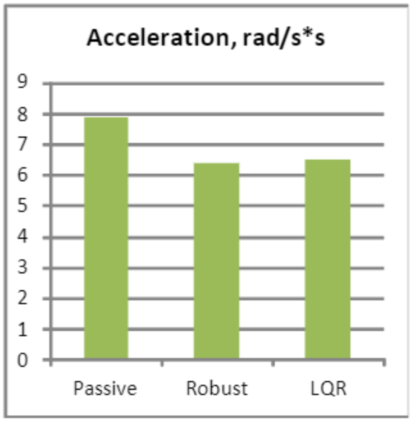

Figure 12: PTP of sprung mass pitch acceleration

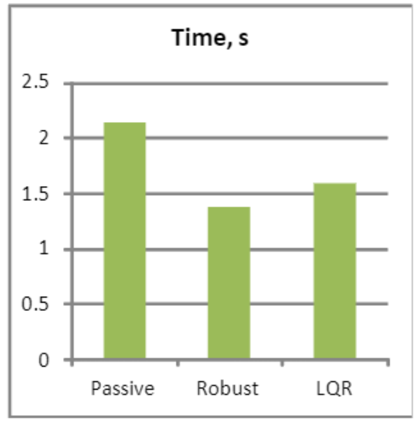

Figure 13: Settling time of sprung mass pitch acceleration

7.2. Suspension Deflection

Figure 14 - Figure 15 shows the suspension deflection of the half car model due to pothole input. The settling time result of front and rear suspension deflection shows that robust controller performance is better than LQR controller and passive system. PTP and settling time of the front suspension show that Robust controller performs 22.8% and 70.4% than passive system in terms of PTP and settling time respectively. On the other hand, robust control performance is slightly better than LQR controller.

Figure 16 and Figure 17 shows the PTP value and settling time of rear suspension deflection performance respectively. Even in this, robust controller performance is better than LQR and passive system. Overall performance of suspension deflection shows passive system has the worst result. It evident from this that, active controllers improves road holding of the car compared to passive system.

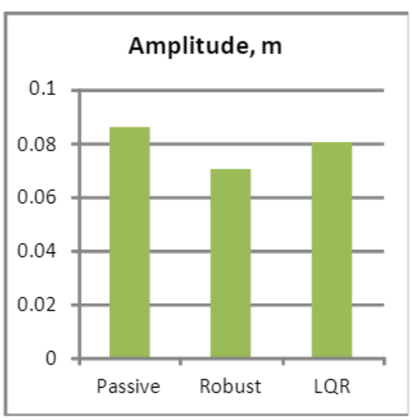

Figure14: PTP of front suspension deflection

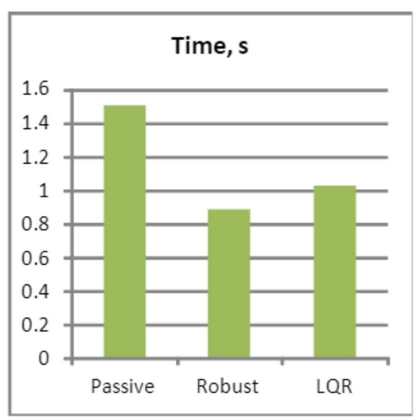

Figure 15: Settling time of front suspension deflection

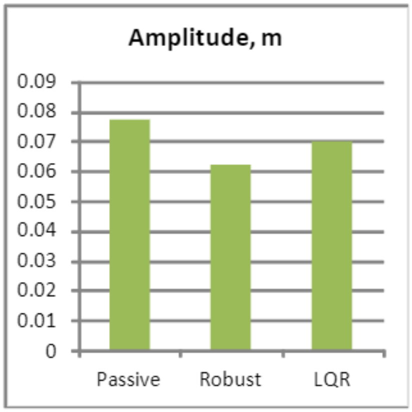

Figure 16: PTP of rear suspension deflection

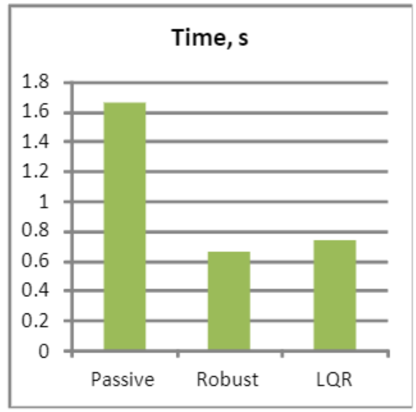

Figure 17: Settling time of rear suspension deflection

7.3. Tire Deflection

Figure18 - Figure 21 shows the summary of front and rear deflection of the system. The result shows that the robust controller has the best PTP value in both the front and rear tire deflection. However, LQR controller proves to perform better than robust control and passive system in terms of settling time. It should be noted that there is significant improvement in performance of active controller when compared to passive system. It is evident from this that robust and LQR control improves road holding of the car significantly. The actual PTP and settling time value of the Robust, LQR controllers and Passive system are shown in Table 5 and Table 6 respectively.

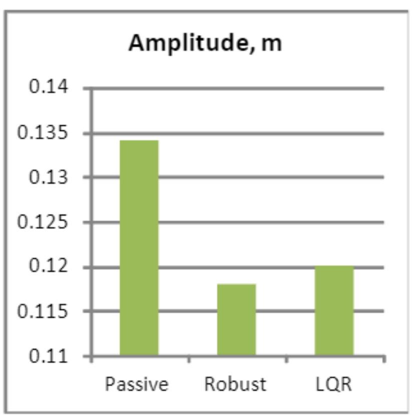

Figure 18: PTP of front tire deflection

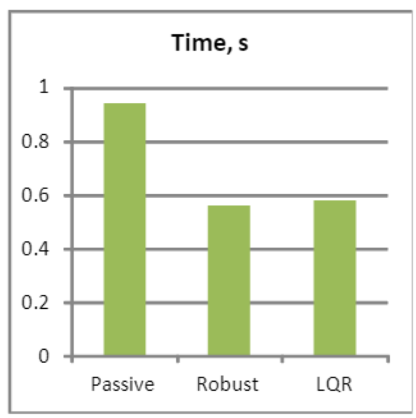

Figure 19: Settling time of front tire deflection

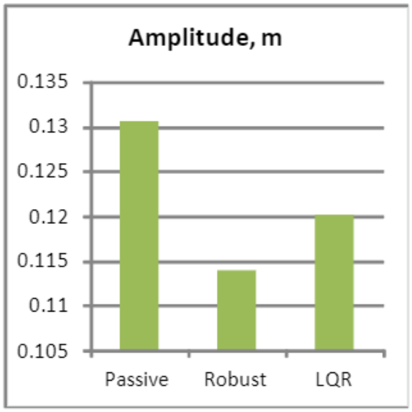

Figure 20: PTP of rear tire deflection

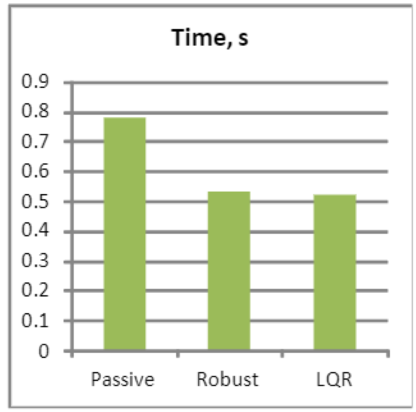

Figure 21: Settling time of rear tire deflection

Table 5: PTP response to pothole input

	Passive	*Robust*	*LQR*
Vertical acceleration (m/s*s)	12.934	10.509	10
Pitch acceleration (rad/s*s)	7.845	6.374	6.5
Front suspension deflection (m)	0.086	0.07	0.08
Rear suspension deflection (m)	0.077	0.062	0.07
Front tire deflection (m)	0.134	0.118	0.12
Rear tire deflection (m)	0.1305	0.114	0.12
Force (kN)	n	1.4	1.36

Table **Error! No text of specified style in document.**: Settling time for pothole input (in seconds, s)

	Passive	*Robust*	*LQR*
Vertical acceleration	1.82	1.21	1.5
Pitch acceleration	2.14	1.37	1.58
Front suspension deflection	1.5	0.88	1.02
Rear suspension deflection	1.66	0.66	0.74
Front tire deflection	0.94	0.56	0.58
Rear tire deflection	0.78	0.53	0.52

8. Response to Random Input

8.1. Sprung Mass Acceleration

Figure22 – Figure 23 shows the RMS value for sprung mass acceleration to random input. The results shows that robust control gives best response for both vertical acceleration and

ISSN: 2005-4238 IJAST

pitch acceleration with 60.7% and 53.3% increase respectively, while LQR controller gives 42.6% and 40.1% increase respectively when compared with passive system.

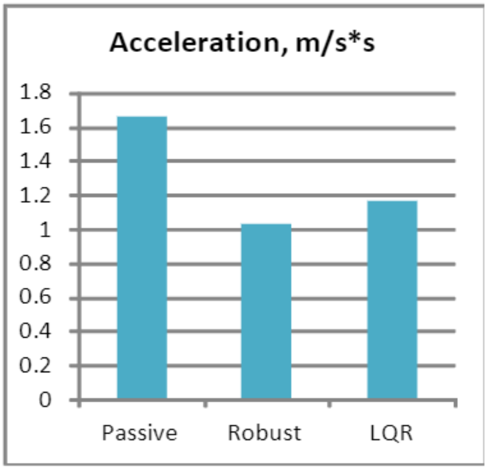

Figure 22: RMS value of vertical acceleration

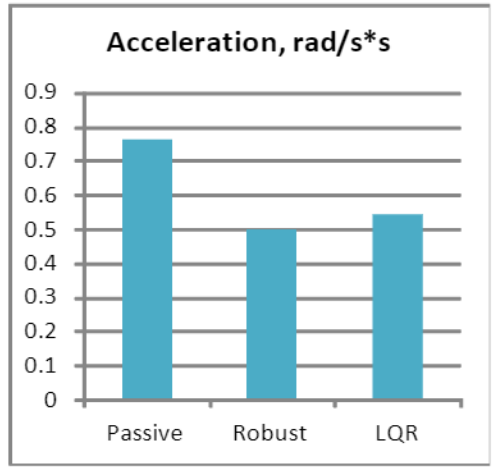

Figure 23: RMS value of pitch acceleration

8.2. Suspension Deflection

Figure24 and Figure25 shows the RMS value of front and rear suspension deflection respectively. In front suspension deflection, robust and LQR controller has similar results which shows 7.7% improvement over passive system. In terms rear suspension deflection, LQR performs better than robust and passive with 18.1% improvement over the later.

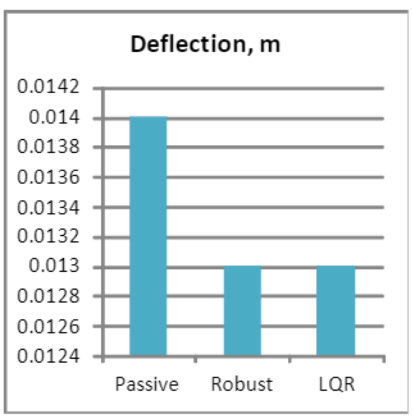

Figure 24: RMS value of front suspension deflection

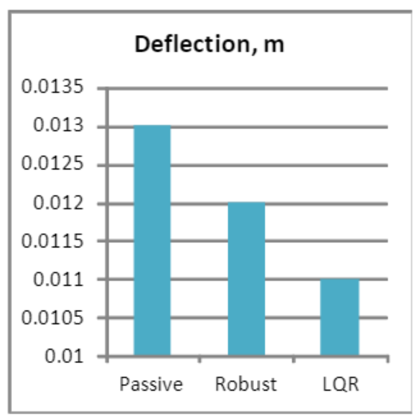

Figure 25: RMS value of rear suspension deflection

8.3. Tire Deflection

Figure26 and Figure 27 shows the summary of RMS value of front and rear tire deflection subject to random input. Again, LQR control proves to perform better than other system. Robust control shows 25% improvement over passive system in front tire deflection. In rear tire deflection, robust and LQR controller has similar performance with 28.5% improvement

ISSN: 2005-4238 IJAST

over passive system. The actual performance value of the Robust, LQR controllers and passive system due to random road is shown Table 7.

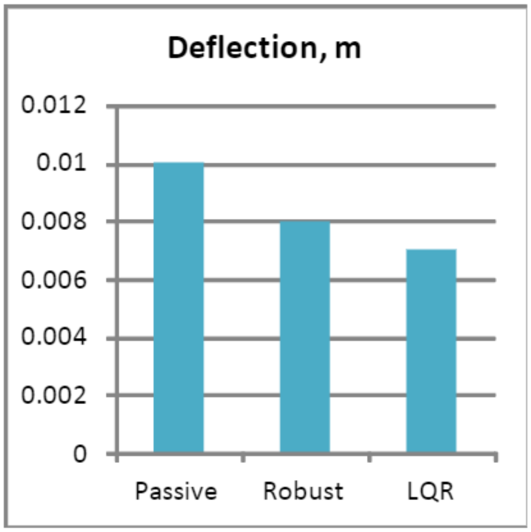

Figure 26: RMS value of front tire deflection

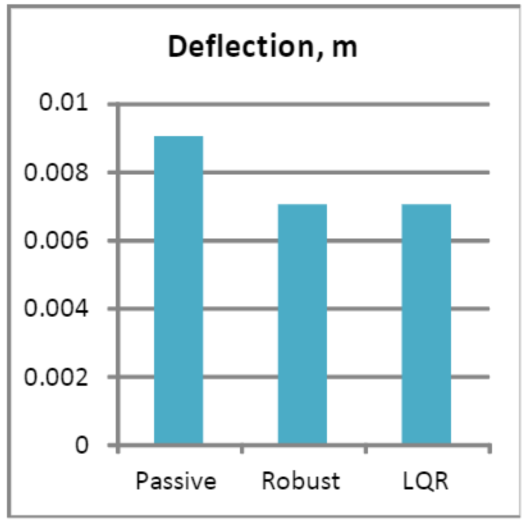

Figure 27: RMS value of rear tire deflection

Table **Error! No text of specified style in document.**: RMS value for random input

	Passive	*Robust*	*LQR*
Vertical acceleration (m/s*s)	1.656	1.03	1.161
Pitch acceleration (rad/s*s)	0.762	0.497	0.544
Front suspension deflection (m)	0.014	0.013	0.013
Rear suspension deflection (m)	0.013	0.012	0.011
Front tire deflection (m)	0.01	0.008	0.007
Rear tire deflection (m)	0.009	0.007	0.007

9. Conclusion

To test the performance of the half car system, two types of controller are used, namely Robust H-infinity control and LQR control. To have the best performance, the weighting parameters of these controllers were optimized using Genetic Algorithm. Result shows that robust controller is able to achieve faster settling time and best PTP performance. It proves that the Improvement in the sprung mass vertical acceleration also leads to the improvement in sprung mass pitch acceleration without compromising the rattle space requirement and road holding performance of the vehicle. The design parameters of both the active controller varies with various road profiles. This proves that particular design parameters in Robust and LQR controller do not have the ability to adapt to the variations in road surface. Furthermore,

ISSN: 2005-4238 IJAST

active controllers significantly improve the performance of the system in all aspects when compared to passive system.

References

[1] A. J. Barr, & Ray, J. I., "Control of an active suspension using fuzzy logic," *Proceedings of the Fifth IEEE International Conference on Fuzzy Systems, 1996. (vol. 1, pp. 42–48). New Orleans, LA,* 1996.

[2] M. Kaleemullah*, et al.*, "Design of robust H∞, fuzzy and LQR controller for active suspension of a quarter car model," in *Mechatronics (ICOM), 2011 4th International Conference On*, 2011, pp. 1-6.

[3] "Can be accessed from," *http://www.armscordi.com/SubSites/Gerotek1/Gerotek01_landing.asp*.

[4] M. Kaleemullah*, et al.*, "Comparative analysis of LQR and robust controller for active suspension," *International Journal of Vehicle Noise and Vibration,* vol. 8, pp. 367-386, 2012.

[5] M. R. Stone, & Demetriou, M. A. , "Modeling and simulation of vehicle ride and handling performance," *Proceedings of the 2000 IEEE International Symposium on Intelligent Control, 2000 (pp. 85–90). Rio Patras.,* 2000.

[6] T. Gillespie, & Karamihas, S., "Simplified models for truck dynamic response to road inputs," *International Journal of Heavy Vehicle Systems, 7(1), 52–63.,* 2000.

[7] A. Soliman, AbdAllah, S. A., El-Beter, A., & Hamid, M, "Effect of suspension spring stiffness on vehicle dynamics," *International Journal of Heavy Vehicle Systems, 8(3), 316–334.,* 2001.

[8] D. Hrovat, "Survey of advanced suspension developments and related optimal control applications," *Automatica,* vol. 33, pp. 1781-1817, 1997.

[9] R. T. Tong, "Ride Control - A Two-State Design for Heavy Vehicle Suspension," *PhD dissertation, University of Illinois at Chicago,* 2001.

[10] Wong, "Theory of Ground Vehicles," *3rd Edition., New York, John Wiley & Sons,* 2001.

[11] 1982, "Reporting Vehicle Road Surface Irregularities," vol. ISO/TC108/SC2/WG4 N57.

[12] A. Capustiac*, et al.*, "A human centered control strategy for a driving simulator," *International Journal of Mechanical & Mechatronics Engineering IJMME-IJENS,* vol. 11, 2011.

[13] Z. Aghaie and R. Amirifar, "H2 and H controllers design for an active suspension system via riccati equations and LMIs," in *2nd International Conference on Innovative Computing, Information and Control, ICICIC 2007, September 5, 2007 - September 7, 2007*, Kumamoto, Japan, 2008.

[14] P. Gu, Konstantinov, "Robuts control design with Matlab," 2005.

[15] K. Zhou and J. C. Doyle, *Essentials of robust control* vol. 104: Prentice Hall Upper Saddle River, NJ, 1998.

[16] B. Boulet, "Robust Control Systems," *Course Notes,* 2007.

[17] F. B. Hasbullah, "Ride Quality Analaysia of Active Suspension Systems for Off-Road Vehicle," *MSc Dissertation, International Islamic University Malaysia,* 2012.